

Research Article

Coalbed Methane Potential Evaluation and Development Sweet Spot Prediction Based on the Analysis of Development Geological Conditions in Yangjiapo Block, Eastern Ordos Basin, China

Xinyu Fu,^{1,2} Yanjun Meng ,^{1,2} Zhongcheng Li,³ Peng Kong,³ Suoliang Chang,^{1,2} Taotao Yan ,^{1,2} and Yanfei Liu^{1,2}

¹College of Mining Engineering, Taiyuan University of Technology, Taiyuan 030024, China

²Shanxi Key Laboratory of Coal and Coal Measure Gas Geology, Taiyuan 030024, China

³China United Coalbed Methane Co. Ltd., Beijing 100016, China

Correspondence should be addressed to Yanjun Meng; mengyanjun15@126.com and Taotao Yan; taotao87225@163.com

Received 3 August 2021; Accepted 4 September 2021; Published 25 September 2021

Academic Editor: Chao Liang

Copyright © 2021 Xinyu Fu et al. This is an open access article distributed under the Creative Commons Attribution License, which permits unrestricted use, distribution, and reproduction in any medium, provided the original work is properly cited.

The evaluation and prediction of favorable coalbed methane (CBM) sweet spot play an important role in well location deployment and recovery prediction in CBM blocks. This work investigates the CBM geology and accumulation characteristics of No. (8 + 9) coal in the Carboniferous Taiyuan Formation in Yangjiapo block based on data from 14 CBM wells. The desorption index is proposed to be used to study the CBM desorption potential in Yangjiapo block, and the parameter of reduced water level is adopted to study the CBM hydrodynamics of the block. Furthermore, the analytical hierarchy fuzzy evaluation method is used to evaluate and prediction the CBM development sweet spot in Yangjiapo block. The results show that the buried depth of the No. (8 + 9) coal seam in Yangjiapo block varies from 693.20 to 1213.20 m, the coal thickness is from 5.40 to 13.10 m, the gas content is from 5.89 to 10.55 m³/t, and the minimum horizontal principal stress is from 9.80 to 20.82 MPa. The desorption potential is better in the southeastern and central-western part of the block. It is found that there is a positive relationship between CBM content and hydrodynamics and indicated that CBM easily concentrates in the lower reduced water level area. The CBM favorable development sweet spot is forecasted to be located in the southeastern part, central-western region, and northeastern part of Yangjiapo block.

1. Introduction

Coalbed methane (CBM) resources are very abundant in China, especially in the Ordos Basin [1]. According to previous studies, the CBM resources in this basin are about 9.62×10^{12} to 10.7×10^{12} m³, accounting for more than 1/4 of the known CBM resources in China [2]. Therefore, researching on the geological conditions of CBM in this basin has important economic significance for the development of CBM in China.

The Yangjiapo block is located in the eastern part of the Linxing area, Hedong coalfield, eastern margin of Ordos Basin (Figure 1). It covers an area of about 150 km² and is

rich in the Permo-Carboniferous coal and CBM resources. During 1998 to 2018, 17 production CBM wells were drilled by the China United Coalbed Methane Corporation, with an average gas production of 1150-1900 m³/day.

So far, only a few literatures have been published on CBM geological research in Linxing area. Most of studies on the CBM in the Linxing area are focused on the geological background and some primary evaluations of CBM reservoirs [3–8]. These data are insufficient to evaluate the CBM development potential and choose the sweet spot area in Yangjiapo block. In this paper, the data from CBM fields and laboratory study are integrated to evaluate the geological controls and CBM development potential in Yangjiapo

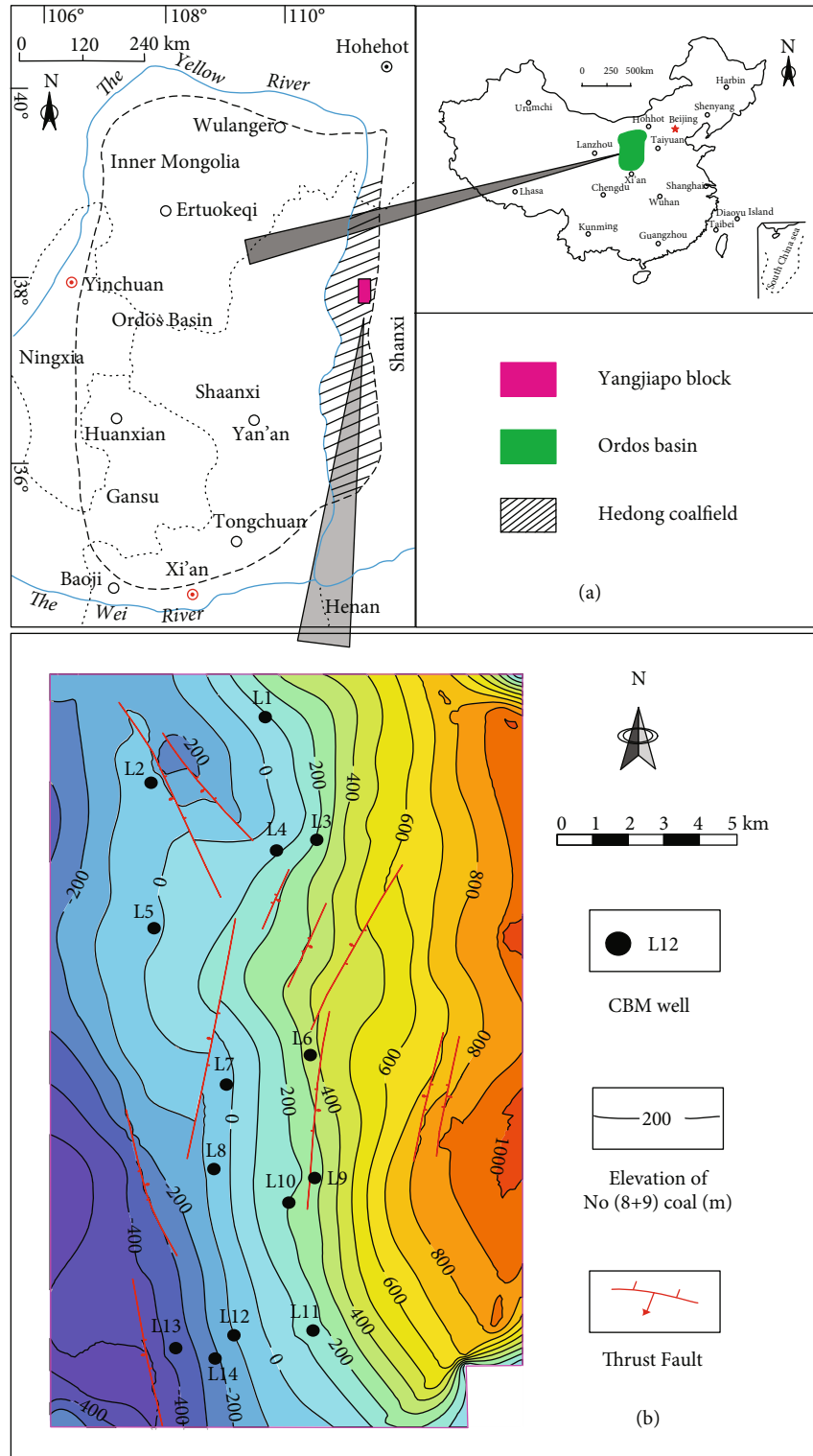


FIGURE 1: (a) Location of the Ordos Basin and Yangjiapo block. (b) Structural elevation of the bottom of No. (8 + 9) coal seam in Yangjiapo block.

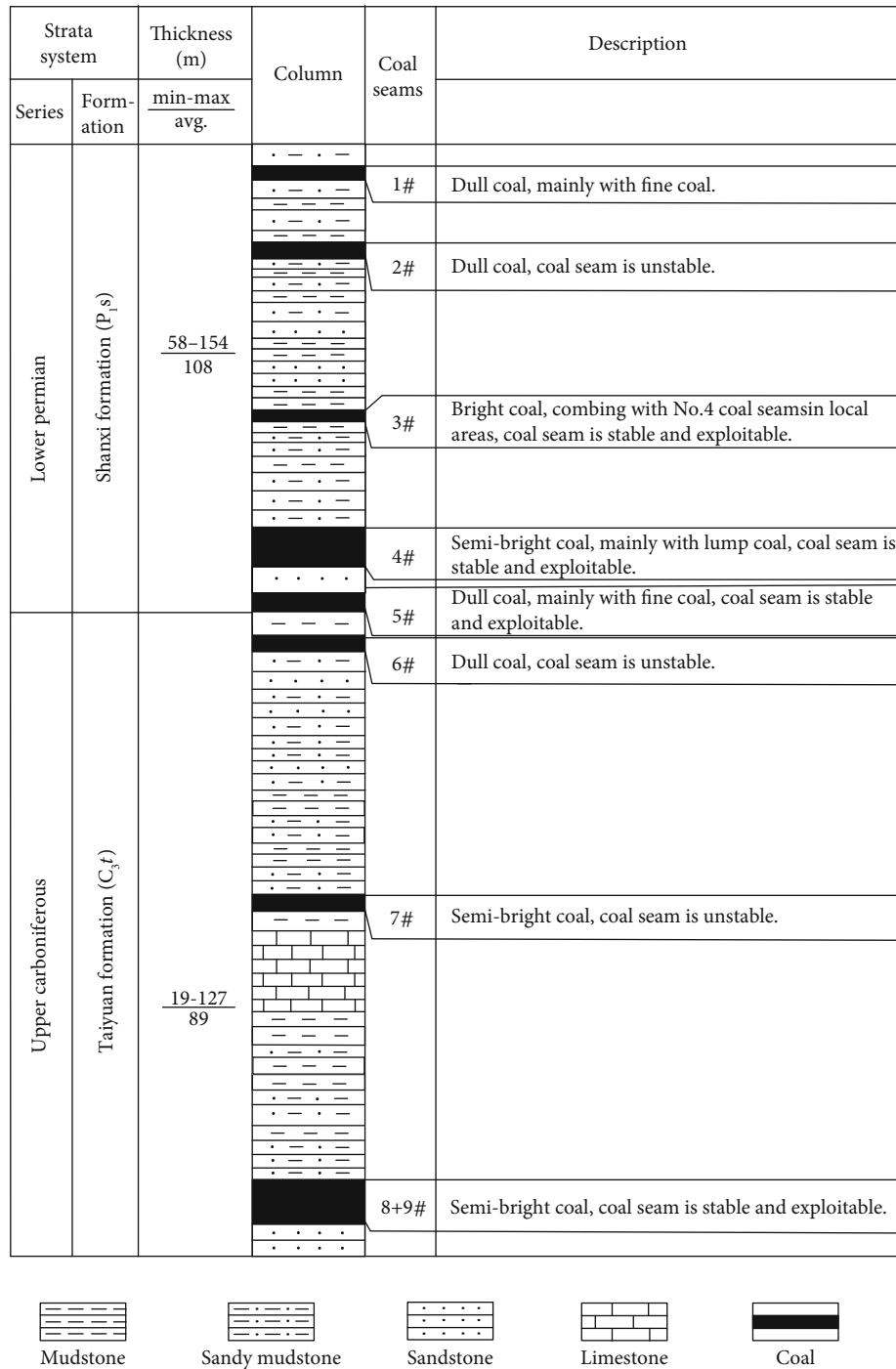


FIGURE 2: Stratigraphic column of Permo-Carboniferous coal-bearing sequences in Yangjiapo block.

block, using analytic hierarchy process (AHP) mathematical models.

2. Geological Setting

2.1. Tectonic Setting. The Ordos Basin, also known as the Shaanxi-Gansu-Ningxia Basin, is a large cratonic basin located in North China with an area of about 371000 km² [9]

(Figure 1). The eastern part of the basin is uplifted and elevated, while the western part is subsided. The basin is further divided into six multiple substructural units and the Hedong coalfield located in Jinxi flexural fold [10, 11]. The Yangjiapo block in northeastern Linxing area is located in western margin of Shanxi anticline of North China Platform, eastern margin of Ordos Basin, and northern Hedong Coalfield. The geologic structure is relatively simple stable in Yangjiapo

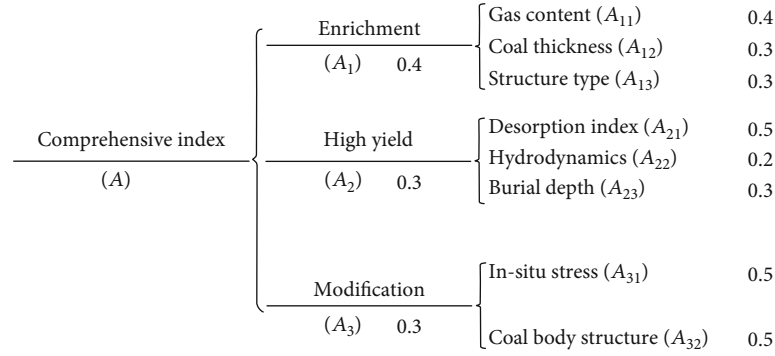


FIGURE 3: The AHP evaluation model with evaluation factors and their weights (numbers in the diagram show the weights in their current hierarchy).

block. The stratum trend is generally north and south, inclined to the west, and the stratum is relatively gentle (Figure 1).

2.2. Coal-Bearing Formations and Coal Seams. The Upper Carboniferous Taiyuan Formation (C_3t) and the Lower Permian Shanxi Formation (P_1s) are the main coal-bearing strata in Yangjiapo block. The Shanxi Formation has a total thickness of 134–153 m with No.1, 2, 3, 4, and 5 coal seams. The Shanxi Formation has a total thickness of 110–149 m and No.6, 7, 8, and 9 coal seams (Figure 2). The No. 8 and No. 9 coal seams, which are often merged together as a unit for No. (8 + 9), are the focus of this study and are also the major minable coal seams. Similar phenomenon occurs in No. 4 and No. 5 coal seams. The Taiyuan Formation was deposited in lagoon and tidal flat facies of marine sedimentary, while the Shanxi Formation was deposited in delta facies of continental sedimentary environment [12, 13].

3. Samples and Methods

3.1. Samples and Experiments. The data used in this study, such as the coal burial depth, coal thickness, gas content, in situ stress, and hydrodynamic data, were obtained from the results of measurements and tests of No. (8 + 9) coal from 14 CBM wells in Yangjiapo block.

Methane adsorption isotherm experiments were performed following the Chinese National Standard GB/T19560-2004. The measurements of gas contents followed the Chinese National Standard GB/T19559-2004, and the reservoir pressure was obtained from injection/fall-off well tests following the Chinese National Standard GB/T24504-2009.

3.2. AHP Model for Evaluating CBM Development Potential. The analytic hierarchy process (AHP) is a structured method based on mathematics and psychology to organize and analyze complex decisions. The fuzzy evaluation object is studied by precise mathematical means, so the fuzzy information is evaluated scientifically, reasonably, and realistically. The method can decompose complex problems into multilevel and multielement, calculate, and judge the same level elements. And it gets the importance of each element to provide decision basis for selecting the optimal scheme.

TABLE 1: Coal burial depth, thickness, minimum horizontal principal stress, gas content, and coal body structure index of No. (8 + 9) coal seam in Yangjiapo block.

Wells	Burial depth (m)	Coal thickness (m)	σ_h (MPa)	Gas content (m^3/t)	F (%)
L1	822.10	12.40	10.33	6.03	63
L2	927.60	8.75	15.60	6.92	20
L3	752.10	12.25	11.20	6.62	65
L4	888.50	13.10	12.61	5.89	8
L5	962.80	5.40	20.82	7.67	74
L6	693.20	11.00	9.97	5.93	20
L7	1062.20	10.30	14.20	8.44	7
L8	1094.50	7.40	14.97	7.41	12
L9	742.10	10.30	9.80	6.14	10
L10	834.78	12.47	12.00	10.55	66
L11	861.95	8.15	15.60	6.70	65
L12	1083.50	7.40	17.64	7.89	60
L14	1213.20	9.00	20.79	5.93	50

Abbreviations: σ_h is the minimum horizontal principal stress and F is the coal body structure index.

The details of the process and principle of the establishment of the AHP model and the possible uncertainties have been discussed in detail in the previous article [14–18]. The AHP evaluation model established in this paper is aimed at CBM development potential evaluation of No. (8 + 9) coal seam in Yangjiapo block and may no longer be effective for other areas or coal seams.

The goal of the AHP evaluation model (Figure 3) is to determine a comprehensive elevation score A (favorable index, value 0–100), which determines the favorable degree of the CBM development. The higher the A score of the first level, the more favorable the CBM development potential obtained. The second level represents three different types of evaluation criteria: the enrichment of CBM with a weight of 0.4 (A_1), the high yield with a weight of 0.3 (A_2), and the modification with a weight of 0.3 (A_3). These three criteria are decomposed into 8 technically alternative parameters (subcriteria) (Figure 3). The determination of the membership degree of the evaluated parameter is another vital

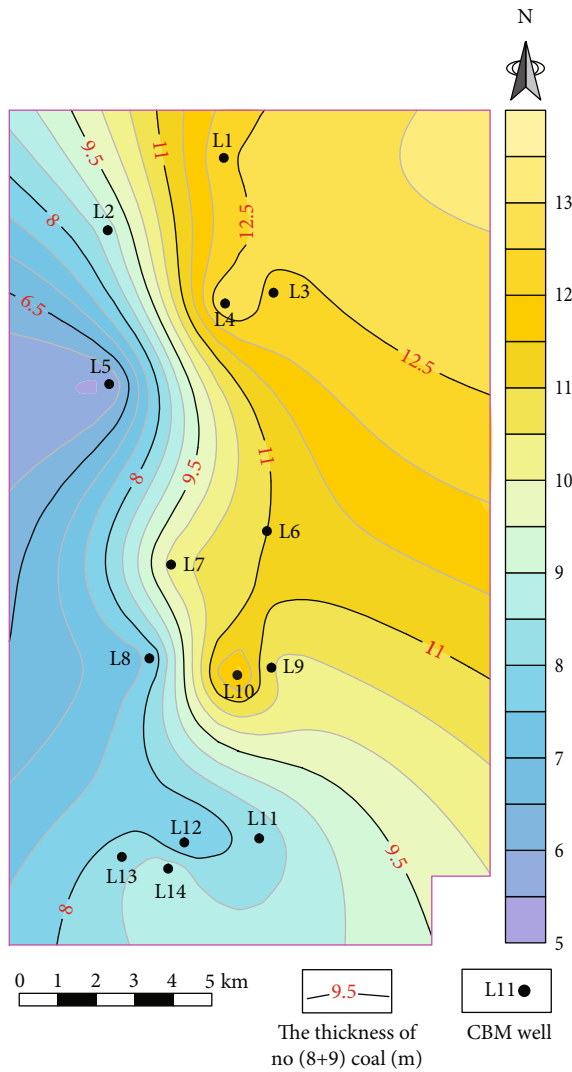


FIGURE 4: Contour map of coal thickness of No. (8+9) coal in Yangjiapo block.

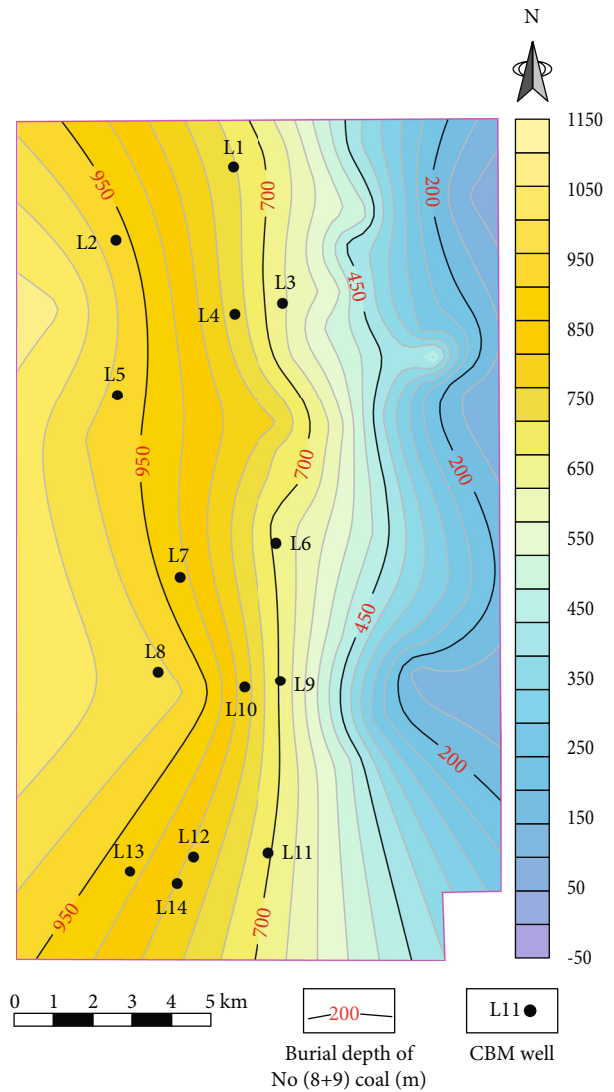


FIGURE 5: Contour map of burial depth of No. (8+9) coal in Yangjiapo block.

process in the evaluation. The details of the membership determination are discussed in Section 4.2 in this paper.

4. Results and Discussions

4.1. Analysis of Development Geological Conditions in CBM Reservoir

4.1.1. Coal Thickness and Burial Depth. In Yangjiapo block, the major seams for CBM exploration and development are No. (4+5) and No. (8+9) coal seams [19, 20]. Based on the data from CBM exploration wells (Table 1), the contour map of No. (8+9) coal seam is shown in Figure 4. The No. (8+9) coal seam has a total minable thickness of 5.40 to 13.10 m (avg. 9.84 m). The coal seam is generally better developed towards the north and east, with the thickest coal seam (up to 13.10 m) in well L4 located in northern Yangjiapo area (Figure 4 and Table 1). And the thick coal seam regions in northern Yangjiapo area are conducive to devel-

opment of multibranch horizontal well CBM (Figure 4), because the coal seams in thick coal seam areas generally have good horizontal continuity, high resource abundance, and stable coal structure. And these advantages can reduce the drilling difficulty and risk of multibranch horizontal well effectively [21].

The coal burial depth which affects the reservoir pressure, permeability, adsorption capacity, and gas content is a very vital geological factor for CBM development [22, 23]. The coal burial depth ranges from 693.20 to 1213.20 m (avg. 918.35 m) (Table 1). To investigate the preservation of coal seams, the coal burial depth of No. (8+9) seam was evaluated using the contour map (Figure 5). The coal burial depth of No. (8+9) coal generally increases from east to west (Figure 5).

4.1.2. Gas Content. The gas content playing an important role in CBM exploration and development can be obtained

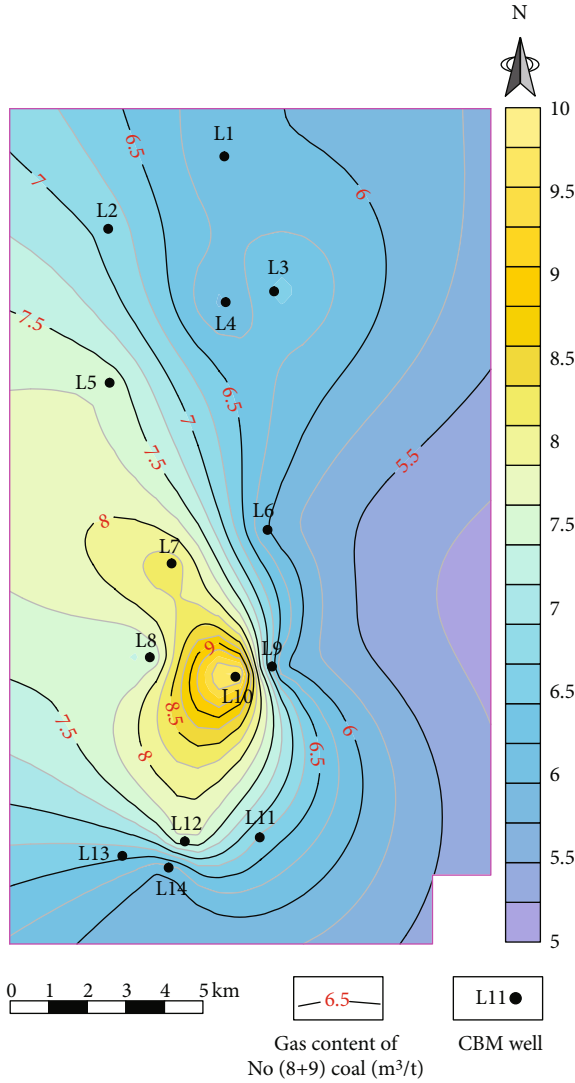


FIGURE 6: Contour map of gas content of No. (8+9) coal in Yangjiapo block.

by direct methods and indirect methods (log analysis, empirical correlations, etc.) [24]. The gas content of No. (8+9) coal in Yangjiapo block ranges from 5.89 to 10.55 m³/t (Table 1). According to the gas content data, the contour map of gas content is drawn. As a result, the gas content generally increases from the east to the west (Figure 6) In the central-southern part (near wells L7, L8, and L10) of the area, the No. (8+9) coal has a relatively higher gas contents (>7.5 m³/t), while in the eastern region of the block, the gas contents is lower (<5.5 m³/t) (Figure 6).

4.1.3. Desorption Capacity. The Langmuir isotherm model is the most used to study adsorption and desorption of methane in coal reservoir. In 2014, Meng et al. proposed the desorption efficiency to quantitatively characterize the desorption rate of CBM under different pressures based on the Langmuir isotherm model [25]. The desorption efficiency, reflecting the gas production rate of CBM wells, is

TABLE 2: Critical desorption pressure, reservoir pressure, desorption efficiency desorption-abandonment difference, and desorption index of No. (8+9) coal seam in Yangjiapo block.

Wells	P_{cd} (MPa)	P (MPa)	η (m ³ /(t MPa))	ΔP (MPa)	D_i (m ³ /t)
L1	1.75	7.42	2.14	1.25	0.63
L2	2.76	8.85	1.10	2.26	0.78
L3	1.83	7.20	2.16	1.33	0.73
L4	1.88	7.59	1.66	1.38	0.57
L5	3.99	8.28	0.78	3.49	1.32
L6	2.03	5.08	1.60	1.53	0.98
L7	2.77	8.48	1.44	2.27	1.07
L8	2.49	9.10	1.50	1.99	0.82
L9	2.22	5.33	1.47	1.72	1.05
L11	6.90	6.75	0.19	6.40	1.23
L12	3.00	9.32	1.23	2.50	0.99

Abbreviations: P_{cd} , critical desorption pressure; P , reservoir pressure; η , desorption efficiency; ΔP , desorption-abandonment difference; and D_i , desorption index.

positively correlated with the productivity of CBM wells. Under the critical desorption pressure, the calculation formula of desorption efficiency is as follows:

$$\eta = V_L \times P_L / (P_{cd} + P_L)^2, \quad (1)$$

where V_L is the Langmuir volume (cm³/g), P_L is the Langmuir pressure (MPa), P_{cd} is critical desorption pressure (MPa), and η is desorption efficiency (m³/(t MPa)).

In 2017, Kang et al. proposed the desorption-abandonment difference to reflect the desorption potential of CBM [26]. The larger the value of desorption-abandonment difference, the greater the desorption potential of CBM wells. The calculation formula of desorption-abandonment difference is as follows:

$$\Delta P = P_{cd} - P_{ad}, \quad (2)$$

where P_{cd} is critical desorption pressure (MPa), P_{ad} is abandonment pressure (MPa), and ΔP is desorption-abandonment difference (MPa).

In this paper, based on the desorption efficiency difference and desorption-abandonment difference, we propose the desorption index to comprehensively reflect the time of gas breakthrough, the amount of desorption, and the desorption potential of CBM wells. The calculation formula of desorption index difference is as follows:

$$D_i = P_{cd} / P \times \eta \times \Delta P, \quad (3)$$

Where P_{cd} is critical desorption pressure (MPa), P is reservoir pressure (MPa), η is desorption efficiency (m³/(t MPa)), ΔP is desorption-abandonment difference (MPa), and D_i is desorption index (m³/t).

The desorption index can reflect the CBM development potential, and the calculation results are shown in Table 2.

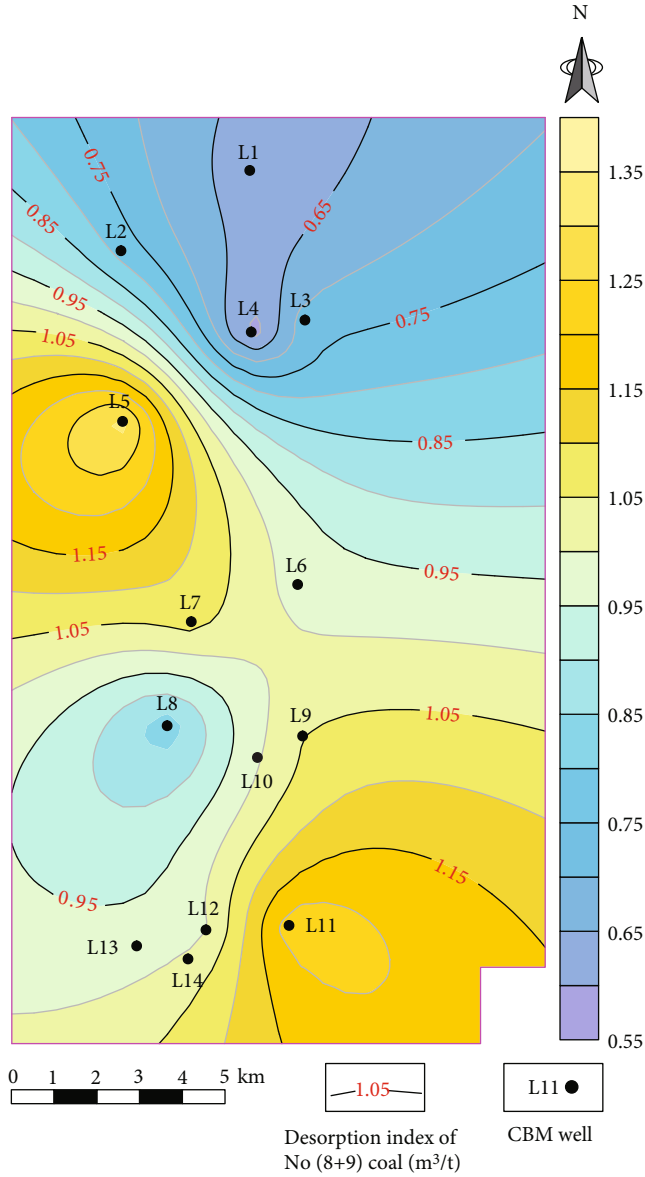


FIGURE 7: Contour map of desorption index of No. (8+9) coal in Yangjiapo block.

According to the calculation results, the contour map of desorption index of the No. (8+9) coal seam is drawn (Figure 7). As shown in the result, the desorption index of the southeastern part (near well L11) of the area and the central-western region (near well L5) of block is higher, which is conducive to the CBM development.

4.1.4. Hydrodynamics and CBM Accumulation. Based on the data of CBM reservoir pressure measured in production practice, an equivalent reduced water level of No. (8+9) coal seam in Yangjiapo block was calculated using the reduced water formula [27, 28].

$$S = H_2 + 10 \times P_c / r_{rwf}, \quad (4)$$

TABLE 3: Reduced water level of No. (8+9) coal seam in Yangjiapo block.

Wells	Reservoir pressure (MPa)	Bottom hole elevation (m)	Reduced water level (m)
L1	7.42	84.60	826.60
L2	8.85	-49.90	835.10
L3	7.20	125.20	845.20
L4	7.59	86.95	845.95
L5	8.28	23.85	851.85
L6	5.08	342.30	850.30
L7	8.48	-44.90	803.10
L8	9.10	-96.50	813.50
L9	5.33	263.75	796.75
L10	6.12	187.70	799.70
L11	6.75	196.22	871.22
L12	9.32	-105.20	826.80
L13	11.66	-378.37	787.63
L14	10.8	-230.26	849.74

where

$$P_c = P + 1/10 \int_{H_1}^{H_2} r_{rw}(H) dH. \quad (5)$$

In this formula, S is the equivalent reduced water level (m), H_1 is the absolute elevation of reservoir pressure (m), H_2 is the elevation of datum level (m), P_c is reduced pressure (MPa), P is reservoir pressure (MPa), r_{rw} is relative density of groundwater (kg/m^3), and $r_{rw}(H)$ is the function of r_{rw} varying with depth.

In the actual calculation, the sea level is used as the datum level, namely $H_2 = 0$. Moreover, the buried depths of CBM wells in Yangjiapo are all less than 1300 m. Within this range of depths, the density of groundwater only has a little change. Therefore, the calculation formula of the converted water level can be simplified as follows [28]:

$$S = 100P + H_1. \quad (6)$$

The calculation results are shown in Table 3. According to the data from reduced water level (Table 3), the contour map of reduced water level of No. (8+9) coal is drawn (Figure 8). Groundwater flows from areas with high reduced water levels to areas with low reduced water level [28]. It can be shown from the figure that the reduced water level in the region decreases from east to west, which reflects that the direction of groundwater flow in the region is mainly from east to west. In general, the groundwater in the western part of the block is recharged from the eastern part of the block. In recharge area in the eastern part of the block, active groundwater reduces CBM content. In the deep groundwater retention area in the western part of the block, the relatively closed groundwater environment is conducive to the enrichment of CBM [27, 29]. This is generally consistent

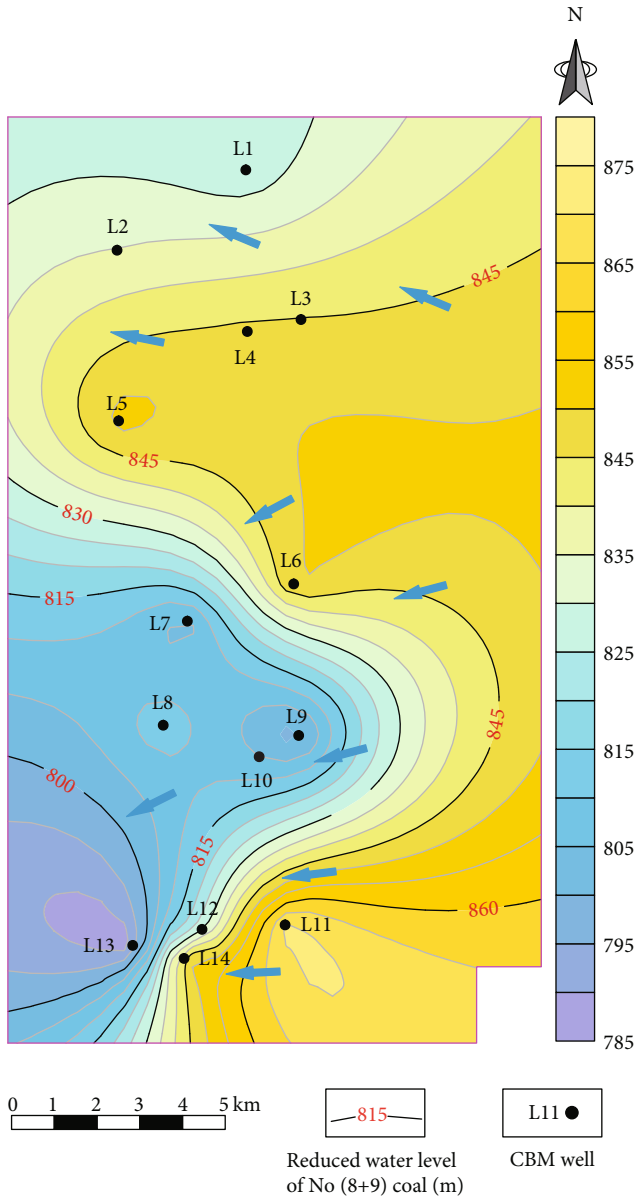


FIGURE 8: Contour map of reduced water level of No. (8 + 9) coal in Yangjiapo block.

with the distribution of gas content (Figure 6) in the No. (8 + 9) coal seam in the region.

4.1.5. In Situ Stress. The in situ stress, as one of the most important geological factors affecting the CBM development, affects the permeability, fracture aperture, morphology, and propagation (direction and dip) of coal reservoir [30]. In situ stress is often measured by the hydraulic fracturing method, which is also appropriate for the in situ stress measurement of coal. The details of this method are discussed in the previous literature [31, 32]. The minimum horizontal principal stress has an important influence on the fracturing pressure and its gradient and also controls the expansion of hydraulic fractures. So this stress is one of the key parameters for CBM development [33]. The contour

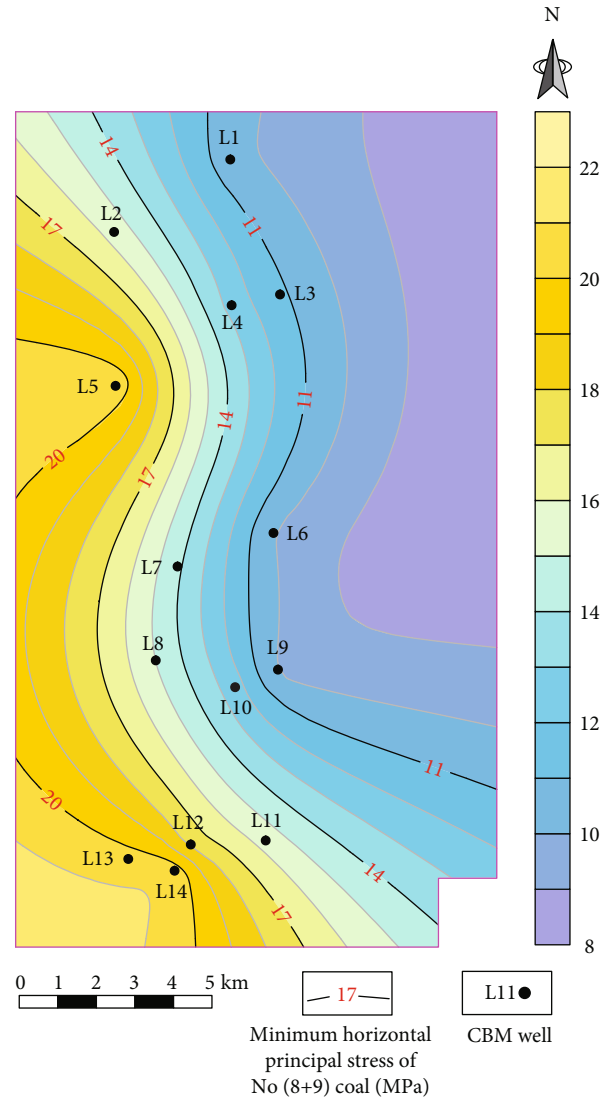


FIGURE 9: Contour map of minimum horizontal principal stress of No. (8 + 9) coal in Yangjiapo block.

map of the minimum horizontal principal stress is obtained by the data (Table 1). The minimum horizontal principal stress of No. (8 + 9) coal generally increases from east to west (Figure 9).

4.1.6. Coal Body Structure Index. Fracturing is an essential measure to increase production of CBM wells, and coal body structure is one of the key factors to determine the fracturing effect [34]. According to the degree of coal body destruction, coal can be divided into primary coal, fragmented coal, granulated coal, and mylonitic coal [35, 36]. Primary coal and fragmented coal have good solidity and poor plasticity, and artificial fractures with great flow conductivity are easily formed through fracturing, which can improve the permeability of coal seams to increase production of CBM. Granulated coal and mylonitic coal have poor solidity and strong plasticity. It is difficult to form main fractures during the fracturing process. The artificial fractures formed have a fast reduction in flow conductivity and a short fracture validity

period, which is not conducive to the increase of CBM well productivity [35]. In this paper, the parameter coal body structure index F is used to quantitatively characterize the degree of coal destruction. The coal body structure index is defined as follows:

$$F = (M_1 + M_2)/M, \quad (7)$$

where M_1 is the thickness of the primary coal, M_2 is the thickness of fragmented coal, M is the thickness of coal, and F is the coal body structure index.

It is significant to note that uncertainties exist when using the estimated coal body structure index. On one hand, the thickness of primary-fractured coal is measured by manual observation, which is uncertain. On the other hand, the coal body structure and thickness of the sample may be affected because of manual coring.

Despite the uncertainties, the coal body structure index can be used to quantitatively characterize the coal structure. The larger the value of F is, the more complete the coal structure is, and the better the fracturing effect is, which is beneficial to increase the productivity of CBM wells. The coal body structure index of the No. (8 + 9) coal in Yangjiapo block is calculated by formula (7) (Table 1). According to the coal structure index data, the isoline map of the coal body structure index is drawn (Figure 10). In the northeastern regions (near wells L1 and L3), central regions (near well L5), and southern regions (near wells L10, L11, and L12), the No. (8 + 9) coal has a relatively higher coal body structure index (>55%), while in central-southern part (near wells L6, L7, L8, and L9) and northwestern area (near wells L2 and L4) of the block, the coal body structure index is lower (<30%) (Figure 10).

4.2. Evaluation and Prediction of CBM Development Sweet Spot Areas

4.2.1. Geological Influence Factors and their Membership.

The membership function is the basic link of fuzzy evaluation. The quality of membership function determines the accuracy of fuzzy evaluation. By establishing the membership function of each evaluation index, the membership of each evaluation index in the study area can be determined, in order to make an objective and comprehensive evaluation of each evaluation parameter and target layer.

The membership function takes values continuously in the range of [0,100], namely, for any element x in the universe U , there is a number $A(x)$ in the range of [0,100] corresponding to it. The membership $A(x)$ is closer to 100, and the degree x belongs to A higher. On the contrary, the membership degree $A(x)$ is closer to 0, and the degree x belongs to A lower.

(1) *Gas Content (A_{11})*. CBM mainly exists on the microporous surface of coal in the form of adsorption, and gas content is one of the main parameters to characterize the enrichment of CBM. The gas content of No. (8 + 9) coal in Yangjiapo block ranges from 5.89 to 10.55 m³/t (Table 1).

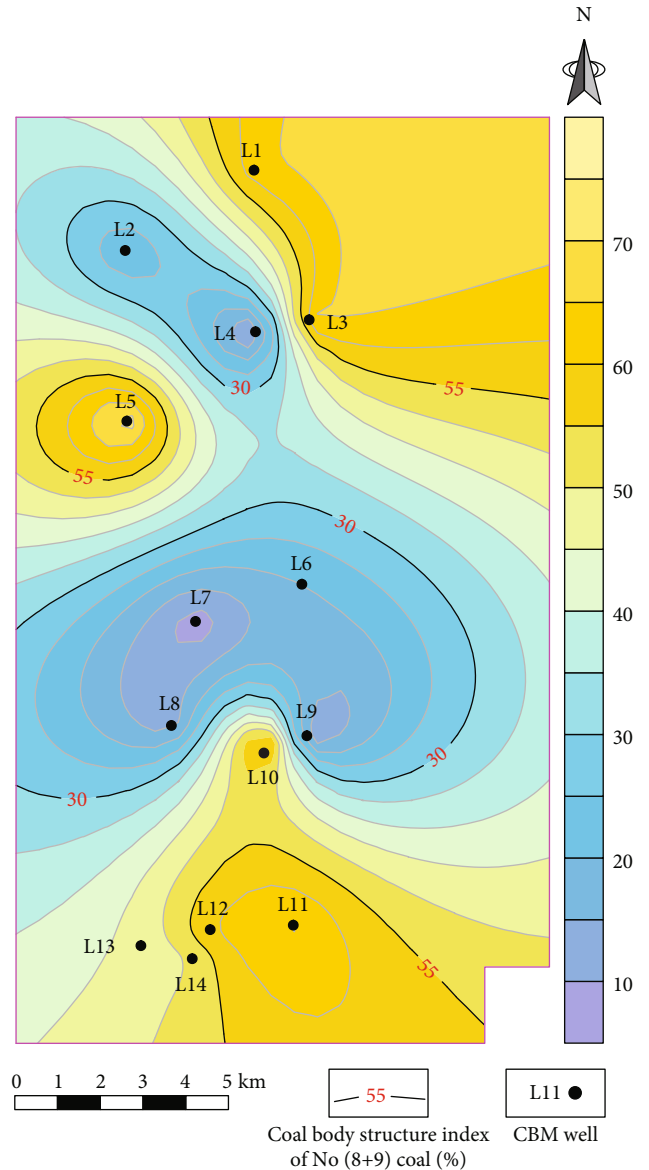


FIGURE 10: Contour map of coal body structure coal index of No. (8 + 9) coal in Yangjiapo block.

For evaluation, the lower and upper thresholds for coal thickness are set at 4 and 8 m³/t, respectively. The parameter of gas content can be rated and scored by the following function.

$$A_{11} \begin{cases} Y = 100, X \geq 8 \\ Y = (X - 4) \times 25, 4 < X < 8 \\ Y = 0, X \leq 4. \end{cases} \quad (8)$$

(2) *Coal Thickness (A_{12})*. The coal thickness used here is the net cumulative coal thickness, which combines the thickness of all mineable coal seams but ignores the thickness of the developed and abandoned coal seams. The coal thickness

TABLE 4: Scoring table for structure type.

Structure type	Simple structures with very few faults	Medium structure with few faults in the area	Complicated structures	Very complicated structures with destructive faults
Value	75-100	50-75	25-50	0-25

of No. (8 + 9) coal in Yangjiapo block ranges from 5.40 to 13.10 m (Table 1). The evaluation function of coal thickness is as follows:

$$A_{12} \begin{cases} Y = 100, Y \geq 8 \\ Y = (X - 3) \times 20, 3 < X < 8 \\ Y = 0, Y \leq 3. \end{cases} \quad (9)$$

(3) *Structure Type* (A_{13}). Structure type is difficult to determine using the quantitative index, so the qualitative method is used to deal with it, and the structural conditions are divided into four levels.

(4) *Desorption Index* (A_{21}). The desorption index can comprehensively reflect the time of gas breakthrough in CBM wells and desorption potential at gas breakthrough. The desorption index of No. (8 + 9) coal ranges from 0.57 to 1.32 m³/t (Table 2). The parameter of desorption index can be assigned by the following function:

$$A_{21} \begin{cases} Y = 100, X \geq 1.5 \\ Y = (X - 0.5) \times 100, 0.5 < X < 1.5 \\ Y = 0, X \leq 0.5. \end{cases} \quad (10)$$

(5) *Hydrodynamics* (A_{22}). The AHP evaluation in this paper uses the reduced water level as the hydrodynamic evaluation parameter, ranging from 787.63 to 871.22 m (Table 3). Considering the importance of varying reduced water level to CBM production and preservation potential, a linear piecewise continuous membership function (11) is used for rating and scoring the parameter of reduced water level.

$$A_{22} \begin{cases} Y = 20, X \geq 850 \\ Y = 100 - (X - 800) \times 1.6, 800 < X < 850 \\ Y = 100, X \leq 800. \end{cases} \quad (11)$$

(6) *Buried Depth* (A_{23}). The buried depth has an important influence on the accumulation and development of CBM. Too large buried depth is not conducive to the desorption of CBM, and too small buried depth will make it difficult

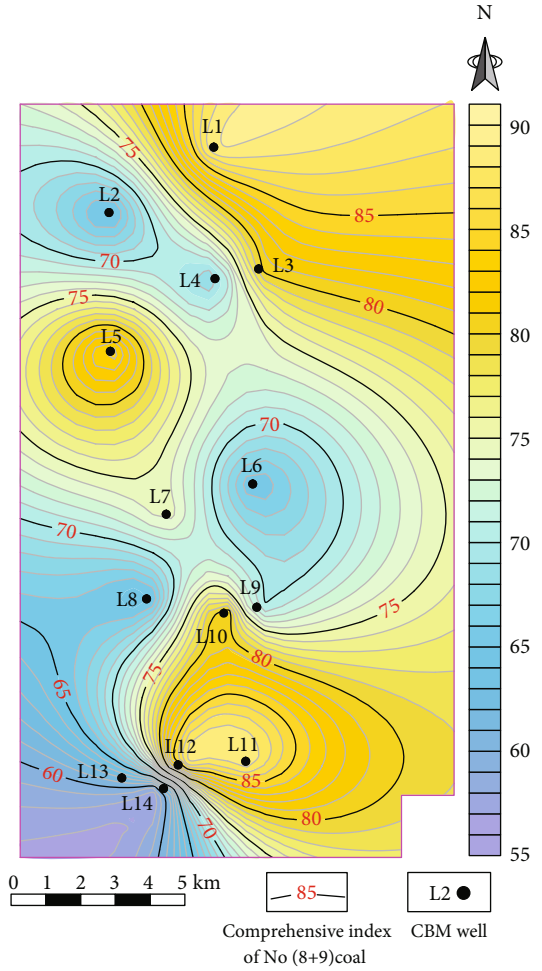


FIGURE 11: Evaluated and predicted result of the CBM development sweet spot in Yangjiapo block.

to preserve CBM. The coal burial depth of No. (8 + 9) coal in block ranges from 693.20 to 1213.20 m (Table 1). The evaluation function of coal buried depth is as follows:

$$A_{23} \begin{cases} Y = 0, X \geq 1200 \\ Y = (1200 - X)/2, 1000 < X < 1200 \\ Y = (X - 600)/4, 600 < X \leq 1000 \\ Y = 0, X \leq 600, \end{cases} \quad (12)$$

(7) *In Situ Stress* (A_{31}). The AHP evaluation in this paper uses the minimum horizontal principal stress as the crustal stress evaluation parameter, ranging from 9.80 to 20.82 MPa (Table 4). The parameter of minimum horizontal principal stress can be assigned by the following function:

$$A_{31} \begin{cases} Y = 0, X \geq 20 \\ Y = 100 - (X - 10) \times 10, 10 < X < 20 \\ Y = 100, X \leq 10. \end{cases} \quad (13)$$

(8) *Coal Body Structure Index* (A_{32}). According to the discussion in Section 4.1.6, the larger the coal body structure index is, the more beneficial the development of CBM is. The coal body structure index of No. (8 + 9) coal in Yangjiapo block ranges from 7% to 74% (Table 1). The evaluation function of coal buried depth is as follows:

$$A_{32} \begin{cases} Y = 100, X \geq 90 \\ Y = (X - 10) \times 1.25, 10 < X < 90 \\ Y = 0, X \leq 10. \end{cases} \quad (14)$$

4.2.2. *Distribution of CBM Sweet Spot for No. (8 + 9) Coal Seam in Yangjiapo Block.* According to the evaluation process in Section 3.2, the CBM development sweet spot for No. (8 + 9) coal seam in Yangjiapo block is shown in Figure 11 (in order to make the comparison of evaluation results clearer, the evaluation scores are enlarged in the same proportion). The high comprehensive index is generally distributed in the northeastern and southeastern parts. The southeastern region (near wells L11 and L12), the northeastern area (near wells L1 and L3), and central-western part (near well L5) of the block are the best development evaluation zones with the highest comprehensive index (>80). However, the central-southern region (near wells L6, L8, and L9), southwestern margin (near wells L13 and L14), and northwestern (near wells L2 and L4) are the poor development evaluation zones with low comprehensive index (<70), which are mainly due to the influence of fault system transformation and low CBM desorption index.

In general, the CBM favorable development sweet spot areas are located in the southeastern, central-western, and northeastern part of Yangjiapo block. In addition, experimental errors and the relatively small data set may have influences on the evaluation results. Nonetheless, the data and information presented here can provide first-order guidance for further CBM exploration and development in Yangjiapo block.

5. Conclusion

- (1) There is a great potential for CBM development from the No. (8 + 9) coals in Yangjiapo block, where the thickness of minable coal seams ranges from 5.40 to 13.10 m, the burial depth of coal seams ranges from 693.20 to 1213.20 m, and the gas content is from 5.89 to 10.55 m³/t. These geological conditions in Yangjiapo block are favorable to the CBM development
- (2) The proposed new parameter desorption index can comprehensively reflect the time of CBM breakthrough, the desorption amount, and the desorption potential of CBM wells in Yangjiapo block. The results show that the desorption index of No. (8 + 9) coal ranges from 0.57 to 1.32 m³/t, and the desorption potential is better in the southeastern and central-western part of the block
- (3) The hydrodynamics in Yangjiapo block is studied using the parameter of reduced water level. It is found that CBM gas content has a positive relationship with hydrodynamics and indicated that CBM is easily concentrates in the lower reduced water level area
- (4) The analytic hierarchy process (AHP) model is used to evaluate the CBM development potential of No. (8 + 9) coal in Yangjiapo block. The results show that the CBM favorable development sweet spot areas are located in the southeastern part, northeastern part, and central-western region of Yangjiapo block.

Data Availability

All data of CBM geology and development are from CBM wells of China United Coalbed Methane Co., Ltd, which are given in the article and described in Acknowledgments.

Conflicts of Interest

The authors declare that they have no conflicts of interest.

Acknowledgments

We are very grateful to China United Coalbed Methane Co., Ltd for helping with the coal sampling and providing some useful data and suggestion for this study. This work was funded by the National Natural Science Foundation (NSFC) Project (41702175, 41902178) and Research Project of China United Coalbed Methane Co., Ltd “*Study on Integration Scheme of Middle Rank CBM in Yangjiapo Block, Eastern Linxing District*” (ZZGSSAYJPYTH2020-300).

References

- [1] S. L. Feng, J. P. Ye, and S. A. Zhang, “Coalbed methane resources in the Ordos basin and its development,” *Geological Bulletin of China*, vol. 21, no. 10, pp. 658–662, 2002.
- [2] X. S. Liu, S. L. Xi, and H. S. Zhou, “Features of upper Paleozoic coalbed methane reservoir in eastern Ordos Basin,” *Coal Geology & Exploration*, vol. 35, no. 1, pp. 37–40, 2007.
- [3] W. Ju, J. Shen, Y. Qin et al., “In-situ stress distribution and coalbed methane reservoir permeability in the Linxing area, eastern Ordos Basin, China,” *Frontiers of Earth Science*, vol. 12, no. 3, pp. 545–554, 2018.
- [4] X. Gao, Y. Wang, X. Ni et al., “Recovery of tectonic traces and its influence on coalbed methane reservoirs: a case study in the Linxing area, eastern Ordos Basin, China,” *Journal of Natural Gas Science and Engineering*, vol. 56, pp. 414–427, 2018.
- [5] Y. Li, D. Tang, P. Wu et al., “Continuous unconventional natural gas accumulations of Carboniferous-Permian coal-bearing strata in the Linxing area, northeastern Ordos basin, China,” *Journal of Natural Gas Science and Engineering*, vol. 36, pp. 314–327, 2016.
- [6] S. X. Zhu, *Study on Prediction of Deep Coalbed Methane Production Capacity and Dynamic Change Law of Reservoir Permeability in Linxing Block*, China University of Geosciences (Beijing), 2020.

- [7] Y. G. Xie, S. Z. Meng, and L. J. Gao, "Assessments on potential resources of deep coalbed methane and compact sandstone gas in Linxing Area," *Coal Science and Technology*, vol. 43, no. 2, 2015.
- [8] L. J. Gao, Y. G. Xie, and X. Z. Pan, "Gas analysis of deep coalbed methane and its geological model for development in Linxing Block," *Journal of China Coal Society*, vol. 43, no. 6, pp. 1634–1640, 2018.
- [9] H. Xu, D. Z. Tang, D. M. Liu et al., "Study on coalbed methane accumulation characteristics and favorable areas in the Binchang area, southwestern Ordos Basin, China," *International Journal of Coal Geology*, vol. 95, pp. 1–11, 2012.
- [10] Y. Li, J. Yang, Z. Pan, S. Meng, K. Wang, and X. Niu, "Unconventional natural gas accumulations in stacked deposits: a discussion of upper Paleozoic coal-bearing strata in the east margin of the Ordos Basin, China," *Acta Geologica Sinica (English Edition)*, vol. 93, no. 1, pp. 111–129, 2019.
- [11] Y. Meng, D. Tang, H. Xu, C. Li, L. Li, and S. Meng, "Geological controls and coalbed methane production potential evaluation: a case study in Liulin area, eastern Ordos Basin, China," *Journal of Natural Gas Science and Engineering*, vol. 21, pp. 95–111, 2014.
- [12] J. H. Zhong, C. Liu, and J. G. Wu, "Symbiotic accumulation characteristics of coal measure gas in Linxing Block, eastern Ordos Basin," *Journal of China Coal Society*, vol. 43, no. 6, pp. 1517–1525, 2018.
- [13] D. Y. Cao, J. Nie, and A. M. Wang, "Structural and thermal control of enrichment conditions of coal measure gases in Linxing block of eastern Ordos Basin," *Journal of China Coal Society*, vol. 43, no. 6, pp. 1526–1532, 2018.
- [14] T. L. Saaty, "Marketing applications of the analytic hierarchy process," *Management Science*, vol. 26, no. 7, pp. 641–658, 1980.
- [15] P. T. Harker and L. G. Vargas, "The theory of ratio scale estimation: Saaty's Analytic hierarchy process," *Management Science*, vol. 33, no. 11, pp. 1383–1403, 1987.
- [16] T. L. Saaty, "How to make a decision: the analytic hierarchy process," *European Journal of Operational Research*, vol. 48, no. 1, pp. 9–26, 1990.
- [17] E. Heo, J. Kim, and K. J. Boo, "Analysis of the assessment factors for renewable energy dissemination program evaluation using fuzzy AHP," *Renewable and Sustainable Energy Reviews*, vol. 14, no. 8, pp. 2214–2220, 2010.
- [18] Y. J. Meng, D. Z. Tang, and H. Xu, "CBM potential productivity assessment through fuzzy mathematics: a case study in Liulin mine area, Hedong coalfield," *Coal Geology of China*, vol. 22, no. 6, pp. 17–20, 2010.
- [19] C. Q. Tao, Y. B. Wang, and X. M. Ni, "Key accumulation period for coal series gas reservoir in upper carboniferous Benxi formation, Linxing block," *Journal of China University of Mining & Technology*, vol. 47, no. 3, pp. 531–537, 2018.
- [20] Z. C. Li, W. F. Du, and J. K. Hu, "Interpretation method of gas content in logging of Linxing block in Ordos Basin," *Journal of China Coal Society*, vol. 43, pp. 490–498, 2018.
- [21] J. Ren, L. Zhang, S. Ren et al., "Multi-branched horizontal wells for coalbed methane production: field performance and well structure analysis," *International Journal of Coal Geology*, vol. 131, pp. 52–64, 2014.
- [22] A. Hildenbrand, B. M. Krooss, A. Busch, and R. Gaschnitz, "Evolution of methane sorption capacity of coal seams as a function of burial history – a case study from the Campine Basin, NE Belgium," *International Journal of Coal Geology*, vol. 66, no. 3, pp. 179–203, 2006.
- [23] L. F. Ruppert, J. C. Hower, R. T. Ryder, J. R. Levine, M. H. Trippi, and W. C. Grady, "Geologic controls on thermal maturity patterns in Pennsylvanian coal-bearing rocks in the Appalachian basin," *International Journal of Coal Geology*, vol. 81, no. 3, pp. 169–181, 2010.
- [24] X. Fu, Y. Qin, G. G. X. Wang, and V. Rudolph, "Evaluation of gas content of coalbed methane reservoirs with the aid of geophysical logging technology," *Fuel*, vol. 88, no. 11, pp. 2269–2277, 2009.
- [25] Y. MENG, D. TANG, X. U. Hao, Q. U. Yingjie, L. I. Yong, and W. ZHANG, "Division of coalbed methane desorption stages and its significance," *Petroleum Exploration and Development*, vol. 41, no. 5, pp. 671–677, 2014.
- [26] Y. S. Kang, J. Wang, and S. Y. Jiang, "Application of quantitative indexes in quantitative evaluation of coalbed methane development potential," *Acta Petrolei Sinica*, vol. 38, no. 6, pp. 677–686, 2017.
- [27] J. Li, B. Wang, and L. Y. Shao, "Hydrogeological zoning and its gas-controlling mechanism: a case study of Baode block, eastern Ordos gas field," *Journal of China University of Mining & Technology*, vol. 46, no. 4, pp. 869–876, 2017.
- [28] B. Wang, F. Sun, D. Tang, Y. Zhao, Z. Song, and Y. Tao, "Hydrological control rule on coalbed methane enrichment and high yield in FZ block of Qinshui Basin," *Fuel*, vol. 140, pp. 568–577, 2015.
- [29] S. Chen, S. Tao, W. Tian, D. Tang, B. Zhang, and P. Liu, "Hydrogeological control on the accumulation and production of coalbed methane in the Anze block, southern Qinshui Basin, China," *Journal of Petroleum Science and Engineering*, vol. 198, p. 108138, 2021.
- [30] Z. P. Meng, J. C. Zhang, and R. Wang, "In-situ stress, pore pressure and stress-dependent permeability in the southern Qinshui Basin," *International Journal of Rock Mechanics and Mining Sciences*, vol. 48, no. 1, pp. 122–131, 2011.
- [31] J. Zhao, D. Tang, H. Xu et al., "Characteristic of in situ stress and its control on the coalbed methane reservoir permeability in the eastern margin of the Ordos Basin, China," *Rock Mechanics and Rock Engineering*, vol. 49, no. 8, pp. 3307–3322, 2016.
- [32] S. H. Tang, "Effect of crustal stress on hydraulic fracturing in coalbed methane wells," *Journal of China Coal Society*, vol. 36, no. 1, pp. 65–69, 2011.
- [33] S. Chen, D. Tang, S. Tao, P. Liu, and J. P. Mathews, "Implications of the in situ stress distribution for coalbed methane zonation and hydraulic fracturing in multiple seams, western Guizhou, China," *Journal of Petroleum Science and Engineering*, vol. 204, p. 108755, 2021.
- [34] Y. B. Yao, H. Wang, and Y. H. Yang, "Evaluation of the hydrofracturing potential for coalbed methane reservoir: a case study of Zhengzhuang CBM field," *Coal Geology & Exploration*, vol. 49, no. 1, pp. 119–129, 2021.
- [35] Y. Wang, D. Liu, Y. Cai, Y. Yao, and Z. Pan, "Constraining coalbed methane reservoir petrophysical and mechanical properties through a new coal structure index in the southern Qinshui Basin, northern China: implications for hydraulic fracturing," *AAPG Bulletin*, vol. 104, no. 8, pp. 1817–1842, 2020.
- [36] Y. Zhang, Y. Meng, P. Hao, Y. Shang, and X. Fu, "Brittleness index of high-rank coal reservoir and its influencing factors in Mabidong block, Qinshui Basin, China," *Geofluids*, vol. 2021, Article ID 5577740, 2021.